

Research article

Use of Eggshell Waste as a source of CaO in Sm³⁺-Doped Na₂O-B₂O₃-CaO-SiO₂ Glass Preparation

Vorrada Loryuenyong*, Suchada Muenna, Supitchaya Thongkaew, Warisara Misamdeang and Achanai Buasri

Department of Materials Science and Engineering, Faculty of Engineering and Industrial Technology, Silpakorn University, Nakhon Pathom, Thailand

Received: 11 August 2022, Revised: 12 October 2022, Accepted: 25 January 2023

DOI: 10.55003/cast.2023.05.23.006

Abstract

Keywords

soda-lime borosilicate glass;
waste;
eggshell;
waste utilization;
luminescence

In this research, calcium carbonate from eggshell waste was used to prepare the soda-lime borosilicate glass samples (Na₂O-B₂O₃-CaO-SiO₂) doped with samarium ions (Sm³⁺) at different Sm₂O₃ concentrations (0, 0.1, 0.2, 0.3, 0.4 and 0.5 mol%). A conventional melt-quenching method at 1,100°C for 3 h was applied in this work to produce the glass samples. The samples were then characterized by XRD, DTA, FT-IR, UV-Vis spectrophotometer and PL techniques. The results showed that the obtained glasses had amorphous structure, and the glass density tended to increase with the addition of Sm₂O₃. The FTIR spectra of the main glass structure revealed that it was composed of trigonal BO₃ and tetrahedral BO₄ borate groups mixing with SiO₄ tetrahedra and non-bridging oxygen. The addition of samarium ions to the glass resulted in a strong orange emission at 562 nm (⁴G_{5/2}→⁶H_{5/2}), 600 nm (⁴G_{5/2}→⁶H_{7/2}), 646 nm (⁴G_{5/2}→⁶H_{9/2}) and 708 nm (⁴G_{5/2}→⁶H_{11/2}) under excitation at 403 nm. The results confirmed that 0.3 mol% Sm₂O₃-doped glass exhibited the highest emission intensity, which suggested that eggshells have a high potential to be used as an alternative CaCO₃-raw material in the production of an efficient luminescent and environmentally-friendly optical electronics material.

1. Introduction

Luminescent glass is a type of optical glass with the active luminescent ions, such as rare earth ions, incorporated into the glass structure. This glass has been used in a wide variety of applications including home decorations and optoelectronics devices such as lasers, light emitting diodes (LEDs), optical fiber cables, etc. When rare earth ions are excited by an incoming energy source, their electrons are raised to an excited state. Once the electrons return to lower energy levels, they

*Corresponding author: Tel.: (+66) 034241708

E-mail: loryuenyong_v@su.ac.th

release the energy in the form of light. Rare earth ions are used extensively because of their intrinsic emission-properties originating from f-f and f-d transitions. The luminescent properties of rare earth ion-doped glass depend on various factors including the type, quality, and concentration of the doping ions. The doping of rare earth ions is, however, based on the use of rare earth oxides. This is because rare earth elements are generally very active with oxygen and readily form oxide compounds.

In order to obtain the optimal luminescent response, the characteristics of the glass matrix is also important. The properties of glasses generally vary with their chemical composition. Two of the most well-known glasses are soda-lime glass and borosilicate glass. While the former is the most common and least expensive type of glass, the latter is more suitable for a wide range of applications requiring high temperature and chemical resistance. Sodium borosilicate glass (and soda-lime borosilicate glass) is the glass system comprising sodium (and calcium) ions acting as glass modifiers together with SiO_2 and B_2O_3 as network formers. This type of glass has numerous applications especially as optical glasses [1]. This is because such glass types have good rare-earth ion solubility [2].

Among the rare earth ions, trivalent samarium ions (Sm^{3+}) have attracted a lot of interest especially in the fields of high-density optical storage and luminescent devices [3]. A strong intense emission band of the Sm^{3+} ions occurs at about 600 nm due to $^4\text{G}_{5/2} \rightarrow ^6\text{H}_{7/2}$ transition, which emits the bright red-orange light under UV and visible-light excitation [2, 4].

Agricultural waste is any waste being generated from different farming processes. The conversion of this kind of waste into other useful materials can be a strategy that adds more value in waste utilization. Eggshell is one of the most common forms of food waste. It typically has a high calcium carbonate (CaCO_3) content (about 94-96% of CaCO_3) [5]. When heated in the temperature range of 800-900°C, eggshell decomposes to form gaseous carbon dioxide and calcium oxide: $\text{CaCO}_3 \rightarrow \text{CaO} + \text{CO}_2$. The gravimetric factor of CaO in CaCO_3 is about 1.787. This process is the same as calcium oxide production from limestone [6]. For the production of glass, calcium carbonate is normally used as a source of CaO due to its stability.

Based on the above concepts, this research studied the preparation of soda-lime borosilicate glasses doped with samarium ions (Sm^{3+}) at different concentrations of Sm_2O_3 ($10\text{Na}_2\text{O}-30\text{B}_2\text{O}_3-10\text{CaO}-(50-x)\text{SiO}_2-x\text{Sm}_2\text{O}_3$, $x = 0, 0.1, 0.2, 0.3, 0.4$ and 0.5 mol%). Eggshells were used as a valuable and sustainable resource of CaCO_3 , which can be used directly or pre-heated to remove undesired components before use. The purpose of this work is to prepare environmentally-friendly types of glass for uses in optoelectronic applications.

2. Materials and Methods

Eggshell wastes were collected from Roti krob Je'Aree (Ratchaburi, Thailand). After washing with tap water several times, the eggshells were fired at 400°C for 4 h to remove organic compounds, crushed into powder using a laboratory ball, and then sieved through an 80 mesh. The obtained eggshell powders were then stored and used as an alternative natural source of calcium carbonate.

Various glasses in the $10\text{Na}_2\text{O}-30\text{B}_2\text{O}_3-10\text{CaO}-(50-x)\text{SiO}_2-x\text{Sm}_2\text{O}_3$ ($x = 0, 0.1, 0.2, 0.3, 0.4$ and 0.5 mol%) system were prepared by the conventional melt-quenching method. Sodium carbonate (Na_2CO_3 , 99.0%), boric anhydride (B_2O_3 , 98.0%), silicon dioxide (SiO_2 , 98.0%), eggshell powder or calcium carbonate (CaCO_3), and samarium (III) oxide (Sm_2O_3 , 99.9%) were first weighed and thoroughly mixed using a mortar and pestle. After all the raw materials were well-mixed, the mixtures were heated up to 1100°C in porcelain crucibles for 3 h. Each sample of molten glass was then poured in a copper mold and annealed at 500°C for 3 h to relieve thermal stress and strain in

the sample. The obtained samples were assigned as SLB0, SLB1, SLB2, SLB3, SLB4, and SLB5, and each were of a different doping concentration.

Another factor that was considered in the preparation procedure was the use of ceramic or alumina crucibles. These crucibles are normally preferred because they are resistant to corrosion and are durable. However, it was reported in previous studies that glass melted in these types of crucibles could be affected by contamination, resulting in lowering of the maximum transmission and IR cut off [7, 8]. Although the presence of contamination from crucibles may be a drawback for optical applications, some contamination from the the crucibles can be beneficial in other applications. It was reported that Al^{3+} ions from alumina (Al_2O_3) could de-cluster several rare earth ions, which diminished the concentration-quenching effect and enhanced emission intensity [8].

To characterize the physical, structural, and optical properties of the obtained soda-lime borosilicate glasses, different characterization techniques were used. The density of the samples was calculated using the Archimedes principle. The weights of the glass samples were measured in air and in water with a 4-digit sensitive microbalance. The molar volume (V_m) was then calculated using the relation $V_m = M/\rho$, where M and ρ are the average molecular weights and densities of the glasses, respectively.

The crystallinity of the obtained glasses was recorded with a Shimadzu diffractometer (LabX XRD-6100 model) with a $\text{Cu K}\alpha$ (1.54 Å) source at room temperature. Fourier transform infrared (FT-IR) spectra were recorded using a Fourier transform infrared spectroscope (Vertex 70, Bruker). Differential thermal analysis (DTA) was carried out at a heating rate of $10^\circ\text{C}/\text{min}$ using a Mettler Toledo TGA/DSC 1 Stare system to determine the glass transition temperatures (T_g) of the obtained glasses. The UV-visible transmission and photoluminescence spectra of the prepared glasses were recorded using a Shimadzu UV-1800 spectrophotometer, and a photoluminescence spectrometer (Avantes, AvaSpec-2048TEC-USB2-2), respectively.

The optical bandgap was calculated by using the Tauc's relation: $\alpha h\nu = B(h\nu - E_g)^n$, where E_g is the optical band gap, h is Planck's constant, ν is the frequency of photons, and B is a constant [9, 10]. The exponent $1/n$ denotes the nature of transitions: $n = 1/2$ for allowed direct band gap transitions, and $n = 2$ for allowed indirect band gap transitions. According to Tauc's relation, the plotting of $(\alpha h\nu)^{1/n}$ versus the photon energy ($h\nu$) gives a straight line in a certain region. The extrapolation of this straight line will intercept the $(h\nu)$ -axis to give the value of the optical energy gap (E_g).

3. Results and Discussion

The XRD patterns of glass samples are shown in Figure 1. There are no crystalline peaks and only broad halo humps observed, which confirms the amorphous nature of glass samples. It is also found that the addition of Sm_2O_3 does not affect the glassy state of the obtained glasses. As shown in Figure 2, FTIR spectra of the glass samples can be divided into four absorption regions. The absorption peak around 462 cm^{-1} is assigned to the vibrations of cations such as the modifier ions (Na^+ , Ca^{2+}) and overlaps with the bending vibration of Si-O-Si of SiO_4 (Q^4). The weak peak at 685 cm^{-1} and the broad band at $1422\text{-}1425\text{ cm}^{-1}$ are associated with the bending vibrations and asymmetric stretching of B-O borate triangles (BO_3), respectively [11-13]. The bands in the region $800\text{-}1200\text{ cm}^{-1}$ are ascribed to the characteristic vibrations of the borate and silicate structural units. The possible silicate groups in this region are associated with non-bridging oxygens (NBOs): Q^4 (Si-O-Si) at 1200 cm^{-1} , Q^3 (Si-O-NBO) at 1075 cm^{-1} , Q^2 (Si-O-2NBO) at 1000 cm^{-1} , and Q^1 (Si-O-3NBO) at 900 cm^{-1} . The presence of non-bridging Si-O groups in the glass structure overlaps with borate groups in the region between $830\text{ to }1109\text{ cm}^{-1}$ [14]. The band near 1000 cm^{-1} is due to the

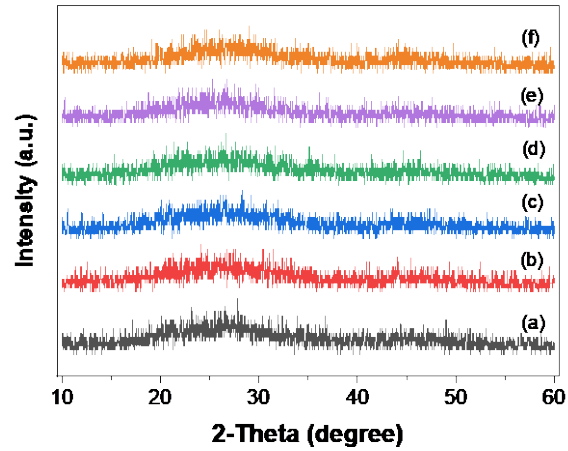


Figure 1. XRD patterns of glasses doped with Sm_2O_3 at different concentrations: (a) SLB0, (b) SLB1, (c) SLB2, (d) SLB3, (e) SLB4 and (f) SLB5

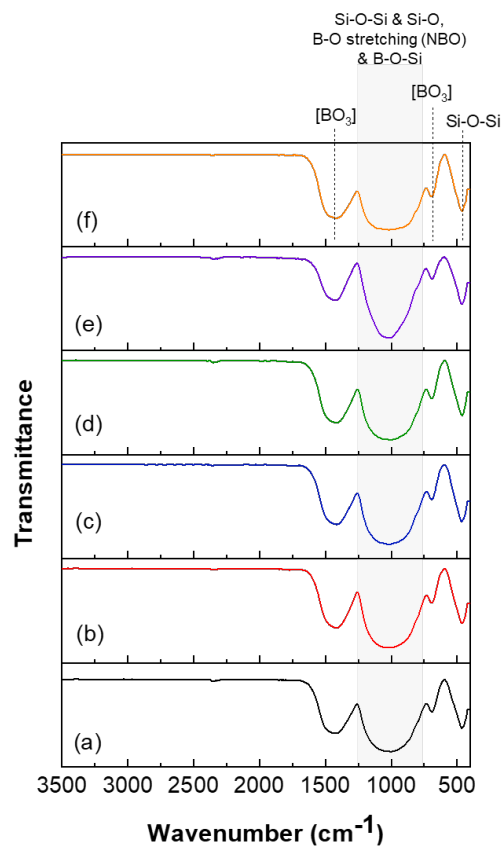


Figure 2. FT-IR spectra of glasses doped with Sm_2O_3 at different concentrations: (a) SLB0, (b) SLB1, (c) SLB2, (d) SLB3, (e) SLB4 and (f) SLB5

asymmetric stretching vibrations of non-bridging B-O-B in BO_4 units, while that between 950-1050 cm^{-1} is due to a stretching vibrations of B-O-Si [15-17]. Generally, in the sodium-borosilicate glass structure, the glass is made up of BO_4 units sharing four oxygen with SiO_4 tetrahedra. The Na^+ ions are used to compensate for the negative charge of the borate units. When Sm^{3+} ions are incorporated into the boron structure, the bridging oxygens are displaced. This leads to an increase in the numbers of non-bridging oxygens (NBOs) and BO_3 units. A small amount of Sm_2O_3 (0.1-0.5 mol%), however, does not affect the glass network, but tends to be incorporated in the interstices, which may break the bridging bonds and create more non-bridging oxygens.

Figure 3 shows the densities and the molar volumes of glasses doped with Sm_2O_3 at different concentrations. The results show that the density increases with increasing Sm_2O_3 concentrations. This is because Sm_2O_3 has a higher molecular weight (348.72 g/mol) than other glass formers such as SiO_2 (60.08 g/mol) and B_2O_3 (69.6182 g/mol). The low density of the undoped glass indicates the presence of a large number of empty interstices. With Sm_2O_3 doping, the molar volume largely decreases, but does not change significantly with increasing Sm_2O_3 concentration. The results suggest that Sm^{3+} ions tend to migrate into the glass structure and fill in any empty interstices, making the structure more compact and giving it nearly constant molar volume.

The DTA analysis of glasses at a heating rate of $10^\circ\text{C}/\text{min}$ is depicted in Figure 4. The results reveal two endothermic peaks, which correspond to the glass transition temperature (T_g) and the melting point (T_m) of the glass samples. The glass transition temperatures of all the samples were measured at the onset of the endothermic peak, as shown in the inset. It can be noticed that the glass transition temperature slightly increased from 572 to 580°C with increasing Sm_2O_3 concentration. Any changes in the thermal stability of the glasses could, generally, be due to many factors such as the formation of non-bridging oxygens or bridging bonds, the chemical bonds, and the packing density in the glass structure [18, 19]. The increase in T_g could be explained by the densification and the packing of the glasses as discussed earlier. There is, however, no evidence of crystallization peaks observed in the results, showing that the obtained glasses doped with Sm_2O_3 are resistant to crystallization.

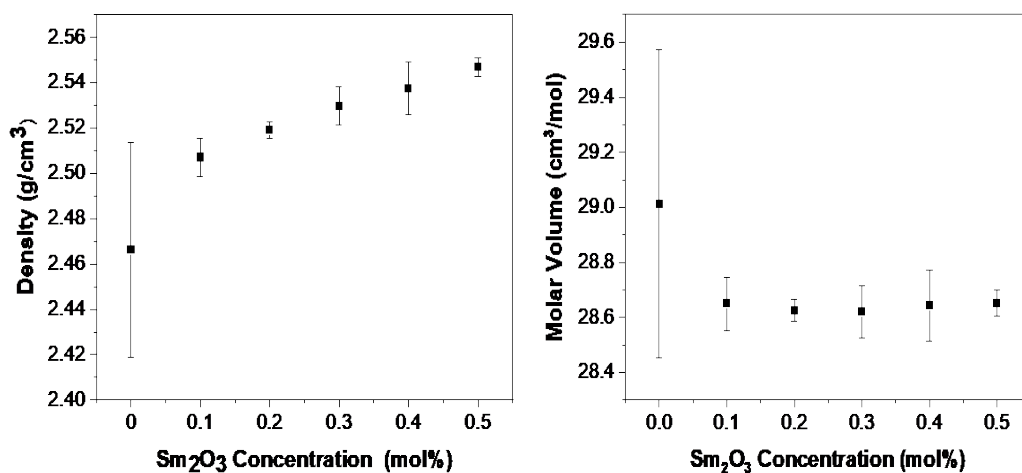


Figure 3. Density and molar volume of glasses doped with Sm_2O_3 at different concentrations

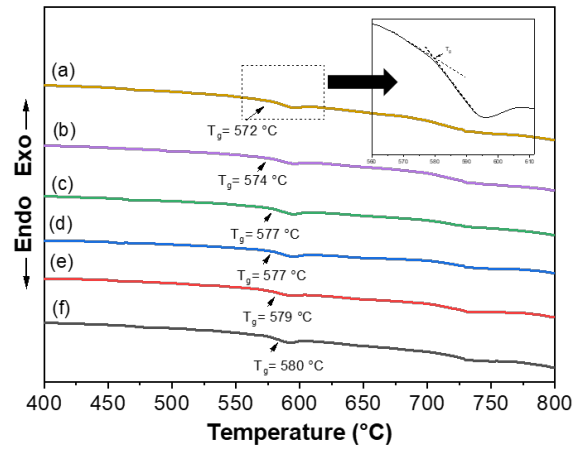


Figure 4. DTA thermograms of glasses doped with Sm_2O_3 at different concentrations: (a) SLB0, (b) SLB1, (c) SLB2, (d) SLB3, (e) SLB4 and (f) SLB5

The UV-Vis transmission spectra are displayed in Figure 5. The parent glass structure shows a strong UV absorption. The addition of Sm_2O_3 leads to light absorption band in the UV-visible region centered at 345, 360, 376, 403, 416, 438, 463 and 472 nm. These correspond to the energy transitions from $^6\text{H}_{5/2}$ to $^4\text{K}_{15/2}$, $^4\text{L}_{17/2}$, $^6\text{P}_{5/2}$, $^6\text{P}_{3/2}$, $^4\text{P}_{5/2}$, $^4\text{G}_{9/2}$, $^4\text{I}_{13/2}$ and $^4\text{I}_{11/2}$, respectively [4]. The highest absorption occurs at 403 nm. Figure 6 shows the optical indirect bandgap (E_g) calculated by using the Tauc relation. From the results, it can be seen that the bandgap energy decreases with increasing concentration of Sm_2O_3 . This may be due to an increase in non-bridging oxygens (NBOs) by incorporating Sm^{3+} into the glass network. The bonding defects in the glass system create more active electrons from the negative charges of oxygen ions in NBOs [20]. These active electrons then accumulate under the valence band energy, causing the valence electrons to move closer to the conduction band energy, thus lowering the bandgap.

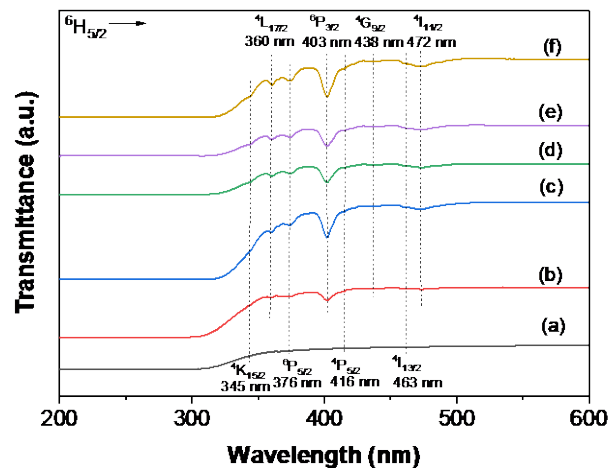


Figure 5. UV-Vis transmission spectra of glasses doped with Sm_2O_3 at different concentrations: (a) SLB0, (b) SLB1, (c) SLB2, (d) SLB3, (e) SLB4 and (f) SLB5

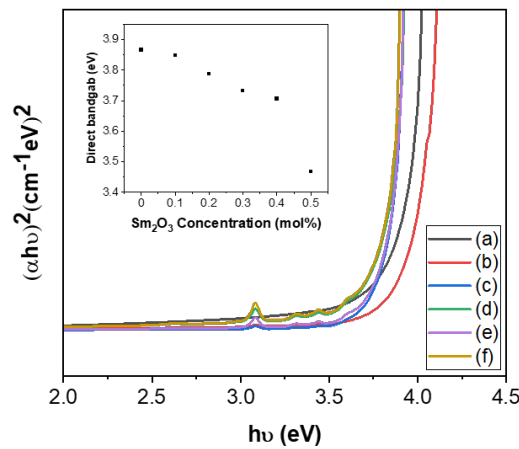


Figure 6. Indirect $(\alpha h\nu)^{1/2}$ vs. $h\nu$ of glasses doped with Sm_2O_3 at different concentrations: (a) SLB0, (b) SLB1, (c) SLB2, (d) SLB3, (e) SLB4 and (f) SLB5

Figure 7 shows the physical characteristics of glass doped with Sm_2O_3 in daylight and under UV light stimulation. It can be seen that the obtained glasses are highly transparent but take on a light-yellow tint with the addition of Sm_2O_3 . Under UV exposure, the doped glasses emit the orange light. Considering the photoluminescence (PL) spectra in Figure 8(a), the emission spectra of the doped glasses show four emission peaks at 562 nm ($^4\text{G}_{5/2} \rightarrow ^6\text{H}_{5/2}$), 600 nm ($^4\text{G}_{5/2} \rightarrow ^6\text{H}_{7/2}$), 646 nm ($^4\text{G}_{5/2} \rightarrow ^6\text{H}_{9/2}$) and 708 nm ($^4\text{G}_{5/2} \rightarrow ^6\text{H}_{11/2}$) when excited at 403 nm. The partial energy diagram of Sm^{3+} -doped glasses is shown in Figure 8(b). It can be observed that the emission intensity is optimal at the wavelength of 600 nm and at the Sm_2O_3 concentration of 0.3 mol% (SLB3). The decrease in the emission intensity at concentrations higher than 0.3 mol% Sm_2O_3 is related to the concentration quenching effects. A high concentration of Sm^{3+} ions can re-absorb the light by itself, leading to a reduction in the luminescence intensity of glass samples [21]. As shown in a CIE diagram (Chromaticity diagram, 1931) of glass samples doped with Sm^{3+} at a concentration of 0.3 mol% (SLB3) (Figure 8(c)), the Sm^{3+} -doped glass gives the orange emission under UV irradiation. The corresponding CIE color coordinate was calculated to be about (0.522,0.474), which is located in the orange region.

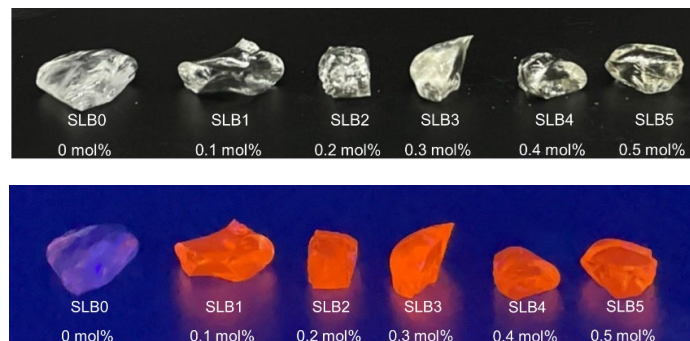


Figure 7. Daylight picture and luminescence images excited by UV light of glasses doped with Sm_2O_3 at different concentrations

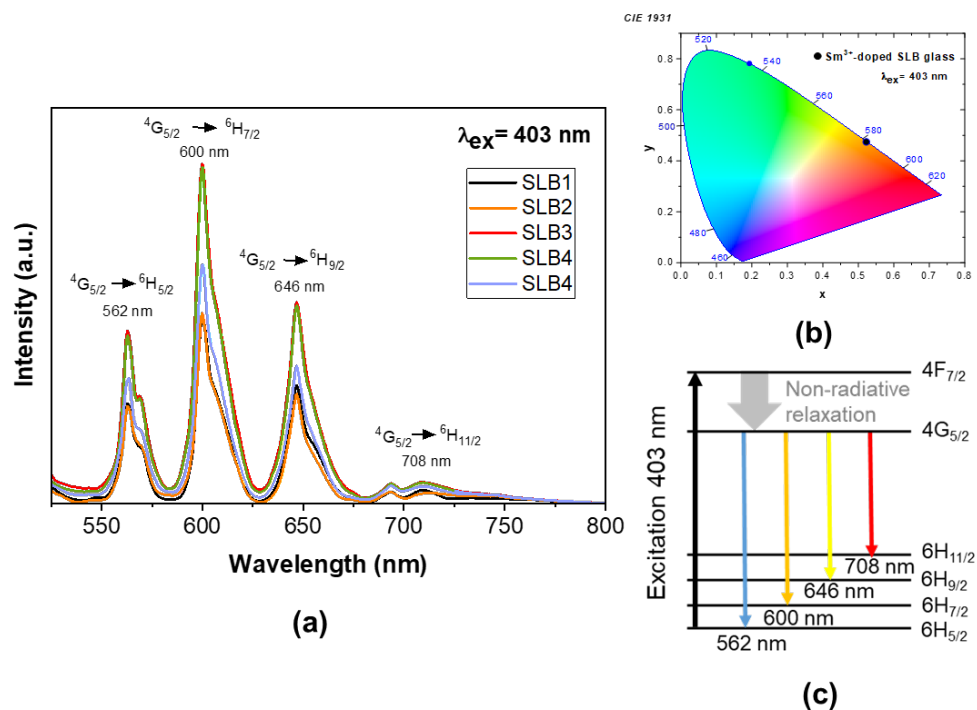


Figure 8. (a) Photoluminescence spectra of glasses doped with Sm_2O_3 at different concentrations, (b) CIE Chromaticity Coordinates under UV irradiation of SLB3 and (c) partial energy level diagram of excitation and emission transitions of Sm^{3+} -doped glasses

4. Conclusions

In this study, $10\text{Na}_2\text{O}-30\text{B}_2\text{O}_3-10\text{CaO}-(50-x)\text{SiO}_2-x\text{Sm}_2\text{O}_3$ ($x = 0, 0.1, 0.2, 0.3, 0.4$ and 0.5 mol%) glasses were prepared by the melt-quenching method with calcined eggshells as a natural source of CaCO_3 . The amorphous nature of the obtained glasses was proven by the presence of broad halos in the XRD patterns. The Sm_2O_3 -doped glasses were found to exhibit higher densities, higher glass transition temperatures, and lower indirect bandgaps. This was due to an increase in packing density of the glass structure and the formation of non-bridging oxygens (NBOs). The emission spectra showed the highest emission intensity occurred at 600 nm (${}^4\text{G}_{5/2} \rightarrow {}^6\text{H}_{7/2}$) and at the concentration of 0.3 mol% Sm_2O_3 , when excited at 403 nm. From CIE 1931 chromaticity coordinates, the emitted light is in the orange region. Based on the results, eggshells could, therefore, be efficiently used to substitute for CaCO_3 in the production of environmentally friendly luminescent glasses.

5. Acknowledgements

The authors wish to thank the Department of Materials Science and Engineering, Faculty of Engineering and Industrial Technology, Silpakorn University for supporting and encouraging this investigation.

References

- [1] Kaewkhao, J., Limsuwan, P. and Ruengsri, S., 2012. Optical characterization of soda lime borosilicate glass doped with TiO₂. *Procedia Engineering*, 32, 772-779.
- [2] Munishwar, S.R., Roy, K. and Gedam, R.S., 2017. Photoluminescence study of Sm³⁺ containing sodium borosilicate glasses and glass-ceramics. *Materials Research Express*, 4(10), DOI: 10.1088/2053-1591/aa8c91.
- [3] Sa-ardsin, W., Discharoen, N., Boonin, K. Yasaka, P. and Kaewkhao, J., 2018. Comparative study of luminescence and optical properties of Sm³⁺ doped glasses with different hosts. *Journal of Thai Interdisciplinary Research*, 13(5), 40-43.
- [4] Wantana, N., Kaewnuam, E., Kim, H.J., Kang, S.C., Ruangtaweep, Y., Kothan, S. and Kaewkhao, J., 2020. X-ray/proton and photoluminescence behaviors of Sm³⁺ doped high-density tungsten gadolinium borate scintillating glass. *Journal of Alloys and Compounds*, 849, DOI: 10.1016/j.jallcom.2020.156574.
- [5] Murakami, F.S., Rodrigues, P.O., De Campos, C.M.T. and Silva, M.A.S., 2007. Physicochemical study of CaCO₃ from egg shells. *Food Science and Technology (Campinas)*, 27(3), 658-662, DOI: 10.1590/S0101-20612007000300035.
- [6] Munawaroh, F., Muharrami, L.K., Triwikantoro, T. and Arifin, Z., 2018. Calcium oxide characteristics prepared from ambunten's calcined limestone. *Jurnal Pena Sains*, 5(1), 65-71, DOI: 10.21107/jps.v5i1.3836.
- [7] dos Santos, I.M.G., Martins Moreira, R.C., de Souza, A.G., Lebullenger, R., Hernandez, A.C., Leite, E.R., Paskocimas, C.A. and Longo, E., 2003. Ceramic crucibles: a new alternative for melting of PbO-BiO_{1.5}-GaO_{1.5} glasses. *Journal of Non-Crystalline Solids*, 319, 304-310.
- [8] Kalpana, T., Gandhi, Y., Sanyal, B., Sudarsan, V., Bragiel, P., Piasecki, M., Kumar, V.R. and Veeraiiah, N., 2016. Influence of alumina on photoluminescence and thermoluminescence characteristics of Gd³⁺ doped barium borophosphate glasses. *Journal of Luminescence*, 179, 44-49, DOI: 10.1016/j.jlumin.2016.06.053.
- [9] Tauc, J., 1968. Optical properties and electronic structure of amorphous Ge and Si. *Materials Research Bulletin*, 3, 37-46, DOI: 10.1016/0025-5408(68)90023-8.
- [10] Mir, F.A., Bhat, G.M., Asokan, K., Batoo, K.M. and Banday, J.A., 2014. Crystal structure, morphological, optical and electrical investigations of Oxypeucedanin micro crystals: an isolated compound from a plant. *Journal of Materials Science: Materials in Electronics*, 25, 431-437.
- [11] Awogbemi, O., Inambao, F. and Onuh, E.I., 2020. Modification and characterization of chicken eggshell for possible catalytic applications. *Heliyon*, 6(10), DOI: 10.1016/j.heliyon.2020.e05283.
- [12] Elbatal, H.A., Hassaan, M.Y., Fanny, M.A. and Ibrahim, M.M., 2017. Optical and FT infrared absorption spectra of soda lime silicate glasses containing nano Fe₂O₃ and effects of gamma irradiation. *Silicon*, 9, 511-517, DOI: 10.1007/s12633-014-9262-7.
- [13] Gaofeng, S., Wu, X., Kong, Y., Cui, S., Shen, X., Jiao, C. and Jiao, J., 2015. Thermal shock behavior and infrared radiation property of integrative insulations consisting of MoSi₂/borosilicate glass coating and fibrous ZrO₂ ceramic substrate, *Surface and Coatings Technology*, 270, 154-163, DOI: 10.1016/j.surfcoat.2015.03.008.
- [14] Kashif, I. and Ratep, A., 2021. Judd-Ofelt and luminescence study of Dysprosium-doped lithium borosilicate glasses for lasers and w-LEDs. *Boletín de la Sociedad Española de Cerámica y Vidrio*, 61(6), 622-633, DOI: 10.1016/j.bsecv.2021.06.001.
- [15] Kumar, V., Rupali, O.P., Pandey, K. and Singh K., 2011. Thermal and crystallization kinetics of yttrium and lanthanum calcium silicate glass sealants for solid oxide fuel cells. *International Journal of Hydrogen Energy*, 36(22), 14971-14976, DOI: 10.1016/j.ijhydene.2011.05.124.

- [16] Bischoe, J. and Warren, B.E., 1938. X-ray diffraction study of sodaboric oxide glass. *Journal of the American Ceramic Society*, 21(8), 287-293.
- [17] Gautam, C., Yadav, A. and Singh A., 2012. A review on infrared spectroscopy of borate glasses with effects of different additives. *International Scholarly Research Notices*, 2012, DOI: 10.5402/2012/428497.
- [18] Raut, A.P. and Deshpande, V.K., 2018. Effect of SiO₂ addition and gamma irradiation on the lithium borate glasses. *Materials Research Express*, 5(1), DOI: 10.1088/2053-1591/aaa2c7.
- [19] Mawlud, S.Q., Ameen, M.M., Md. Sahar, R. and Ahmed, K.F., 2016. Influence of Sm₂O₃ ion concentration on structural and thermal modification of TeO₂-Na₂O glasses. *Journal of Applied Mechanical Engineering*, 5(5), DOI: 10.4172/2168-9873.1000222.
- [20] Reddy, Y.L.P., Waaiz, M. and Reddy, C.V.K., 2017. Optical properties of fluoroborate glasses doped with Samarium(Sm³⁺). *International Journal of Pure and Applied Physics*, 13(2), 249-257.
- [21] Mirdda, J.N., Mukhopadhyay, S., Sahu, K.R. and Goswami, M.N., 2022. Enhancement of optical properties and dielectric nature of Sm³⁺doped Na₂O-ZnO-TeO₂ Glass materials. *Journal of Physics and Chemistry of Solids*, 167, DOI: 10.1016/j.jpcs.2022.110776.